RSC Medicinal Chemistry

ROYAL SOCIETY OF CHEMISTRY

RESEARCH ARTICLE

View Article Online
View Journal

Cite this: DOI: 10.1039/d5md01025j

Revealing deamidation and isoaspartate formation during peptide analysis, purification and storage by tandem mass spectrometry

V. Erckes, L. Chamera Rendueles, A. Misiek and C. Steuer *

Interest in peptides and peptidomimetics continues to grow, particularly in the context of drug discovery and development. However, spontaneous chemical modifications such as deamidation and isoaspartate formation present significant challenges, as they are difficult to detect and can compromise peptide integrity and function. Conventional chromatographic methods and standard mass spectrometric analyses often fail to distinguish structurally similar peptides with nearly identical physicochemical properties and masses. In this study, tandem mass spectrometry (MS/MS) was employed to monitor deamidation events involving asparagine, glutamine and C-terminal amide functional groups. Both collision-induced dissociation (CID) and electron-transfer dissociation (ETD) were systematically evaluated and could differentiate the resulting species without relying on chromatographic separation, with ETD further enabling semi-quantitative detection of deamidation and isoaspartate formation. Using this approach, we confirmed isoaspartate formation under mildly basic conditions such as phosphate-buffered saline, whereas amidated peptides remained stable in neutral aqueous–organic mixtures or at lower temperatures. In contrast, exposure to acidic conditions, particularly in the presence of the additive trifluoroacetic acid, as commonly used during HPLC purification, resulted in substantial direct deamidation by hydrolysis without detectable isoaspartate formation. Notably, this degradation showed clear site dependence, with especially C-terminal amides, being markedly more susceptible in our study. These findings underscore how readily deamidation and isoaspartate formation can occur under routine laboratory conditions and highlight the utility of CID and ETD mass spectrometry for reliably detecting these modifications. The study emphasizes the need for careful analytical monitoring during peptide synthesis and purification to avoid misinterpretation of structural integrity.

Received 16th November 2025,
Accepted 24th December 2025

DOI: 10.1039/d5md01025j

rsc.li/medchem

1. Introduction

Peptides play a central role in many physiological processes and have gained increasing attention as drug candidates. They offer a favourable balance of target specificity and binding affinity relative to their molecular size, and their pharmacokinetic properties can be tuned, driving interest in their therapeutic use.[1–4] However, even subtle changes, including unintended single-site chemical modifications or differences in counterions, can markedly alter peptide properties.[5] Among the most relevant modifications are deamidation and isoaspartate (isoAsp) formation.[6] Deamidation converts an amide to a carboxylic acid, introducing a negative charge at physiological pH, whereas isoAsp formation alters the peptide backbone *via* a β-linkage that inserts an extra methylene group. Both degradation processes have been shown to affect stability, activity, immunogenicity, and therapeutic efficacy of peptides and proteins, making them relevant across all stages of peptide drug discovery and development.[7–11] For deamidation in peptides two main pathways may be considered, as shown in Fig. 1.[12] Direct hydrolysis is a water-assisted cleavage of an amide group to give the corresponding carboxylic acid, which is typically favoured under acidic conditions (pH ≤ 4) and accelerated by increased temperature. Direct hydrolysis can affect any accessible amide bond in Asn or Gln side chains as well as an amidated C-terminus. In contrast, the succinimide (aspartimide) mechanism is side-chain-specific that applies primarily to Asp and Asn. In this pathway, the backbone amide nitrogen of the residue following Asp/Asn attacks the Asp/Asn side-chain carbonyl to form a five-membered succinimide intermediate, which is generally the rate-determining step. Subsequent hydrolytic ring opening yields a mixture of aspartate and isoaspartate, often enriched in isoAsp, with the exact ratio sequence- and condition-dependent.[13] The succinimide pathway is generally favored at neutral to mildly alkaline pH (approx. 7–9) and accelerated by

Laboratory of Pharmaceutical Analytics, ETH Zurich, Institute of Pharmaceutical Sciences, Zurich, Switzerland. E-mail: christian.steuer@pharma.ethz.ch

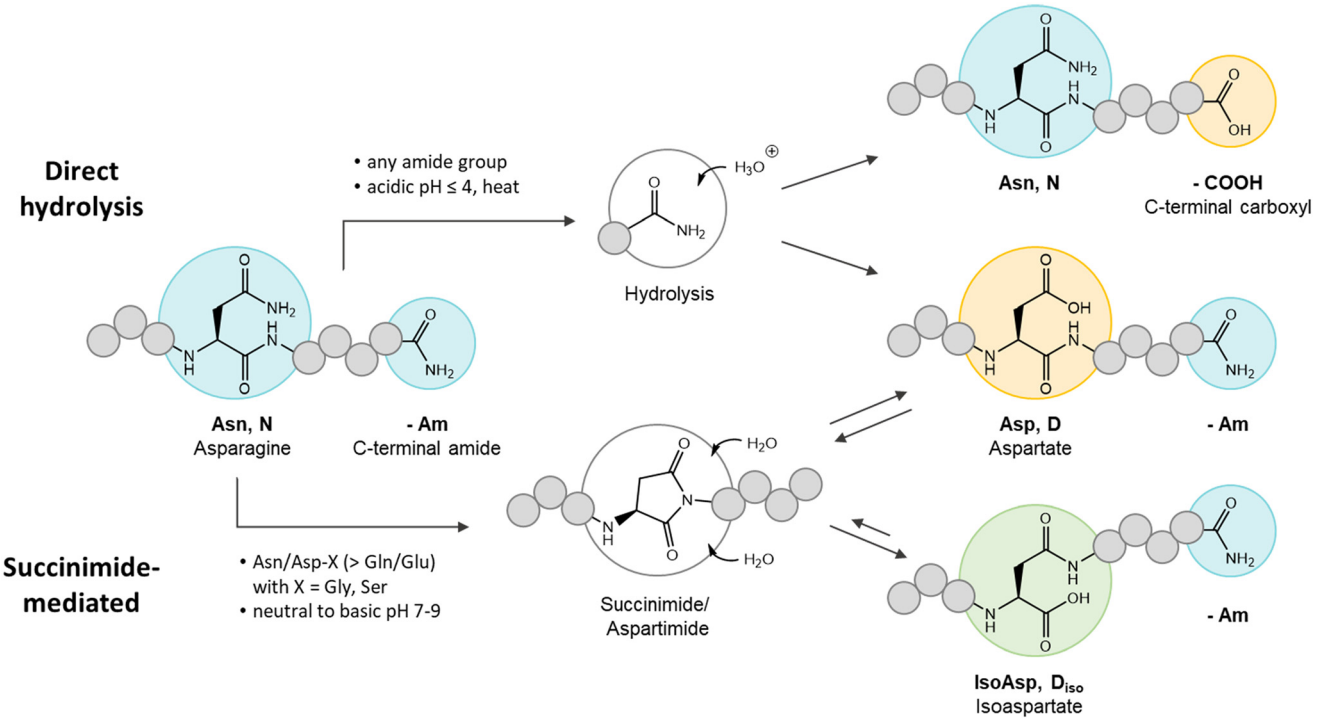

Fig. 1 Schematic representation of direct hydrolysis and succinimide-mediated degradation leading to deamidation and isoaspartate formation in amino acid sidechains of Asn. Amide functional groups are highlighted in blue, carboxylic acids in orange, and isoaspartate is highlighted in green.

flexible sequence motifs (*e.g.* Asn-Gly and Asn-Ser).[14] By contrast, Gln deamidation *via* a glutarimide intermediate is slower because the formation of the six-membered ring is less favourable kinetically.[13] In solid-phase peptide synthesis, basic deprotection steps can promote aspartimide formation, whereas appropriate protecting-group strategies can reduce this side reaction.[15]

Analytically, distinguishing deamidation products remains challenging.[6] A +0.984 Da mass shift places deamidated species close to the M + 1 isotopic peak of the amide precursor (difference approx. 0.019 Da), requiring high resolving power and mass accuracy to avoid misassignment.[16–18] Moreover, Asp and isoAsp are isobaric, so precursor mass alone cannot differentiate them. Reversed-phase LC often provides only subtle retention differences, and partial co-elution can complicate quantification.[6] Tandem mass spectrometry (MS/MS) can provide additional information, by localizing modifications along the backbone based on specific fragmentation ions.[19,20] Collision-induced dissociation (CID) predominantly yields b/y-ions and can localize a +1 Da shift to a single amino acid in the peptide.[21] Distinguishing isoAsp from Asp by CID is very limited and peptide-dependent with reported ions such as $b + H_2O$ and $y - 46$ not universally reliable.[22–24] Electron transfer dissociation (ETD) as an alternative fragmentation technique to CID yields mainly c/z ions.[21,25] ETD can generate isoAsp diagnostic ions ($c + 57$, $z - 57$), which arise from the altered backbone connectivity in isoAsp.[26,27] ETD performance however, requires sufficiently high precursor charge states for fragmentation efficiency.

Although deamidation and isoAsp formation are well documented under physiological and synthetic conditions, much less is known about their relevance during routine peptide purification, analysis, and storage, where peptides are frequently exposed to aqueous–organic mixtures, varying pH, and elevated temperatures. Due to the similarity in chemical properties these modifications are not straightforward to detect, making them easy to overlook. The aim of this study was to develop a practical workflow that enables semiquantitative detection of deamidation and isoAsp formation without relying on baseline chromatographic separation. Using a model peptide containing both a side-chain amide in Asn and a C-terminal amide, we evaluate how commonly used solvents and storage conditions influence deamidation and then extended the analysis to additional sequences to compare the specific susceptibilities of Asn, Gln, and C-terminal amides. Our goal was to translate MS/MS analysis into a practical guidance on how to find deamidation and isoAsp and under which purification, analysis, or storage conditions they are most likely to arise.

2. Material and methods

2.1 Chemicals

Acetonitrile (ACN) and methanol (MeOH) for LC-MS analysis (OPTIMA, LC-MS grade) was obtained from Fisher Chemicals (Loughborough, UK). Nanopure water was used from an in-house ELGA Purelab water purification system (VWS, Celle, Germany). Sodium chloride (NaCl, ≥99.5%), trifluoroacetic

acid (TFA, ≥99%), triisopropylsilane (TIS) and formic acid (FA; 98.0–100%), were purchased from Sigma Aldrich (Buchs, Switzerland). 0.1 M hydrochloric acid (HCl) solution, 0.1 M sodium hydroxide (NaOH) solution and acetic acid (AA, Emsure Supelco, Ph. Eur.) were obtained from Merck (Darmstadt, Germany). 25% ammonia solution (Anal R, NORMAPUR) was purchased from VWR chemicals (PA, USA). *N*,*N*-Diisopropylethylamine (DIPEA) was obtained from ROTH (Karlsruhe, Germany).

2.2 Solid phase peptide synthesis

Peptides, listed in Table 1 were synthesized by Fmoc solid phase peptide synthesis. Detailed synthesis and purification protocols are provided in the SI. Isoaspartate (D_{iso}) was introduced to the sequence using L-Fmoc-aspartic acid alpha-*t*-butyl ester as a building block. For all peptides stock solutions at a concentration 0.1 mM were prepared in water.

2.3 Liquid chromatography coupled to electrospray ionization and tandem mass spectrometry (LC-ESI-MS/MS)

2.3.1 LC-ESI-MS. Peptide separation was performed on a Waters Acquity UPLC equipped with a Zorbax Eclipse Plus C18 column (2.1 × 50 mm, 1.8 μm particle size, Agilent, USA). Solvent A was 0.1% FA in water, and solvent B was 0.1% FA in ACN. Gradient elution was tested starting at 95% or 98% A for 2 min, followed by an increase in B at 10% min^{-1}, 5% min^{-1}, 1% min^{-1}, or 0% min^{-1} (isocratic elution) with a flow of 0.5 mL min^{-1} at 25 °C. Each run was followed by 5 min of re-equilibration to the starting conditions. Compounds were ionized with a heated electrospray ionization probe (HESI-II, Thermo Scientific, USA). The heater temperature was set to 0 °C (corresponds to approx. 50 °C operating temperature), sheath gas flow rate to 34 arbitrary units (arb), auxiliary gas flow rate to 11 arb, sweep gas flow rate to 0, spray voltage to 5 kV, capillary temperature to 275 °C, capillary voltage to 31 V and tube lens to 80 V. MS detection was carried out on an LTQ XL ion trap mass spectrometer (Thermo Scientific, USA). Full MS scans were recorded from *m*/*z* 100–1200 at normal scan rate, positive polarity, and profile data type. The AGC target for full scans was set to 1.50×10^{04}. This method was used to acquire MS spectra or coupled with targeted or data dependent MS/MS analysis.

2.3.2 Targeted MS/MS. Targeted fragmentation was performed at *m*/*z* 365.70, corresponding to the $[M + 2H]^{2+}$ ion of the Pep1(D)-Am peptide, with an isolation width of 1.0 *m*/*z*. CID was conducted using helium as collision gas with an AGC target of 5.00×10^{03}. CID activation was performed with a normalized collision energy of 35, an activation *Q* of 0.25 and an activation time of 30 ms. ETD was performed with fluoranthene (*m*/*z* 202) as a reagent ion. A minimum fluoranthene signal intensity of $>10^6$ (negative mode) was ensured prior to ETD analysis. ETD parameters were set to emission current 50.00 μA, electron energy −80 V, CI gas pressure 30 psi, source temperature 160 °C, vial 1 temperature 108 °C, restrictor temperature 160 °C and transfer line temperature 160 °C. ETD activation was performed with an activation time of 100 ms and an AGC target of 1.00×10^{05}.

2.3.3 Data dependent MS/MS. Data dependent acquisition of fragment spectra was configured to allow the automated non-specific generation of fragment spectra of multiple analytes with distinct masses. As a first scan event, a full scan with normal scan rate and a scan range from 100–1200 *m*/*z* was performed. Data was acquired in positive polarity with the data type profile. In a second scan event, ions for fragmentation were selected starting from the most intense ion detected in the first scan event with a minimum signal threshold of 2000 counts within 300–1200 *m*/*z* and an isolation width of 1.0 *m*/*z*. To allow the generation of fragment spectra of multiple charged species, dynamic exclusion was enabled. Settings for dynamic exclusion were as follows: repeat count 2, repeat duration 15 s, exclusion list size 150, exclusion duration 8 s and exclusion mass width ±0.5 *m*/*z*. Fragment spectra were acquired in positive polarity at a normal scan rate with the data type centroid and a default charge of 3 within a mass range of 110–1200 *m*/*z*.

2.4 Semiquantitative method for the analysis of deamidated and isoaspartate peptides

A total peptide concentration of 0.1 mM was used in all experiments, with an injection volume of 5 μL unless stated

Table 1 Peptides for LC-MS/MS method development. Theoretically expected masses of single and multiple protonated charged ions of the peptide were calculated with PICKAPEP[28]

Name	Peptide[a]			Molecular weight (Da)	MS detection (*m*/*z*)	
	N-term	Sequence	C-term		$[M + H]^+$	$[M + 2H]^{2+}$
Pep1(N)-Am ([a])	H–	RLL**N**ASG	**–NH_2**	728.85	729.4371	365.2225
Pep1(N)-OH ([a])	H–	RLL**N**ASG	–OH	729.84	730.4212	365.7145
Pep1(D)-Am ([a])	H–	RLL*D*ASG	**–NH_2**	729.84	730.4212	365.7145
Pep1(D_{iso})-Am ([a])	H–	RLLD_{iso}ASG	**–NH_2**	729.84	730.4212	365.7145
Pep1(D)-OH ([a])	H–	RLL*D*ASG	–OH	730.82	731.4052	366.2065
Pep1(D_{iso})-OH ([a])	H–	RLLD_{iso}ASG	–OH	730.82	731.4052	366.2065
Pep1(Q)-Am	H–	RLL**Q**ASG	**–NH_2**	742.88	743.4528	372.2303

[a] Used for method development of semiquantitative LC-ESI-MS/MS method. Abbrev.: N-term = N-terminus, C-term = C-terminus; underlined: basic functional groups, bold: possible deamidation site, italic: possible site for isoaspartate formation.

otherwise. The Pep1 series (Table 1) was used to establish a semiquantitative LC-ESI-MS/MS workflow capable of distinguishing amidated, deamidated, and isoaspartate-containing species. For method development, an equal mixture of Pep1(N)-Am, Pep1(N)-OH, Pep1(D)-Am, Pep1(D_{iso})-Am, Pep1(D)-OH and Pep1(D_{iso})-OH was analyzed by LC-ESI-MS testing different gradients. Each peptide was also analyzed individually by data dependent LC-ESI-MS/MS (CID and ETD) using a 1% min^{-1} gradient to obtain reference retention times and MS/MS spectra. To evaluate whether chromatographic peak area could be used for relative quantification where LC separation was achieved, binary mixtures of Pep1(N)-Am and Pep1(D)-Am were analyzed, and the relationship between mole fraction and peak area was assessed. To identify fragment ions capable of distinguishing co-eluting species with identical precursor *m*/*z*, pairwise CID and ETD spectra of Pep1(D)-Am *vs.* Pep1(N)-OH and of Pep1(D)-Am *vs.* Pep1(D_{iso})-Am. Spectra were compared using volcano plot analysis of $[M + 2H]^{2+}$ precursor ions to identify statistically significant differences between fragment-ion intensities. Binary mixtures of Pep1(D)-Am with Pep1(N)-OH or Pep1(D_{iso}) in varying ratios were then analyzed to evaluate the linearity of candidate diagnostic ions. Finally, mixtures containing all six Pep1 variants were used to assess robustness with respect to injection volume and composition. LC-resolved species were quantified by peak area, while the contributions of co-eluting species were estimated from diagnostic fragment-ion intensities.

2.5 Stability studies

Pep1(N)-Am was incubated at 40 °C for 7 days under the following conditions: H_2O, H_2O : ACN (1 : 1), H_2O : MeOH (1 : 1), 10 mM HCl, 0.1% FA, 0.1% AA, 0.1% TFA, 0.2% TFA, 5% TFA, 50% TFA, 95% TFA, 100% TFA, 95/2.5/2.5 TFA/TIS/H_2O, 95/5 TFA/TIS, 10 mM NaOH, 0.1% NH_3, 0.1% DIPEA, 10 mM NaCl and PBS (pH 7.4). Temperature-dependent stability was investigated in 0.1% TFA at −20 °C (freezer), 4 °C (fridge), 20 °C (room temperature) and 60 °C. For −20 °C stability testing underwent one freeze–thaw cycle per time point (4 freeze thaw cycles in total) with each 1 h thawing at room temperature. Pep1(D)-Am, Pep1(N)-OH, Pep1(D)-OH and Pep1(Q) were incubated at 40 °C for 7 days at 0.2% TFA. Samples were collected at time points 0, 24, 48, 96 and 168 hours. Each sample with an initial concentration of 0.4 mM was diluted 1 : 20 in water (0.02 mM) and analyzed with an injection volume of 10 μL in triplicate by targeted LC-ESI-MS/MS (CID, ETD), except for Pep1(Q)-Am samples the untargeted LC-ESI-MS/MS (CID, ETD) method was used.

2.6 Data processing

MS and MS/MS data were acquired and extracted using XCalibur (4.4.16.14, Thermo Fisher Scientific) and converted to mzML with msConvert.[29,30] Data analysis was performed in Python[31] (3.10.10). Chromatograms and MS spectra were processed using pyOpenMS[32] and MOCCA2.[33] Statistical analyses were carried out with NumPy[34] (1.23.5), pandas[35] (1.5.3) and SciPy[36] (1.15.3). Data visualization was performed using matplotlib[37] (3.10.1). Chemical structures were drawn using ChemDraw (20.0.0.41).

3. Results and discussion

3.1 Development and performance of a semiquantitative LC-ESI-MS/MS workflow for deamidation and isoaspartate analysis

The peptides in the Pep1 series differed only in C-terminal modification (amide *vs.* acid) or in the identity of a single residue (Asn, Asp, or isoAsp), providing a controlled system for monitoring deamidation and isoAsp formation. All peptides were obtained at >94% purity except Pep1(D)-OH, which was retained for method development (Fig. S1–S3, Table S1). Initial LC optimization indicated that shallow gradients and high aqueous starting conditions improved separation, but under the final method (98% H_2O, 1% min^{-1} gradient), Pep1(N)-OH, Pep1(D)-Am, and Pep1(D_{iso})-Am remained co-eluting (Fig. 2A) and shared the same $[M + 2H]^{2+}$ *m*/*z*. Thus, chromatographic retention and precursor mass alone were insufficient for differentiation. Where species were baseline-separated (*e.g.*, Pep1(N)-Am *vs.* Pep1(D)-Am), LC peak areas scaled linearly with relative content (Fig. S4), supporting their use for relative quantification. For the co-eluting triplet, adding fragmentation provided the required specificity. Fragmentation experiments were performed on the doubly charged precursor, as singly protonated peptides containing strongly basic residues, such as Arg in our case, can exhibit altered fragmentation behavior that complicates spectral interpretation.[38,39] CID spectra of Pep1(D)-Am and Pep1(D_{iso})-Am were largely overlapping, whereas Pep1(N)-OH showed distinctive C-terminal fragments. ETD generated additional structure-informative ions, including characteristic isoAsp fragments. Comparison with calculated fragment ions, consistent with established peptide fragmentation pathways,[40] and volcano-plot comparison of replicate CID/ETD spectra identified multiple fragment ions with reproducible differences between peptide pairs (Table S2). These candidates were evaluated in binary mixtures, where the ETD $(c3 + 57)^+$ showed best performance for isoAsp, providing a linear response even at low Pep1(D_{iso})-Am levels with an $R^2 > 0.95$. For Pep1(N)-OH, the ETD $c5^+$ ion showed the strongest linear correlation. An example ETD spectrum of the mixture of Pep1(D)-Am, Pep1(D_{iso})-Am, and Pep1(N)-OH highlighting these fragments is shown in Fig. 2B, and corresponding linear fits of diagnostic ions is shown in Fig. 2C. Based on these results, the final workflow combined (i) integration of the extracted-ion chromatogram (*m*/*z* 364.5–367.5) for LC-resolved species and (ii) deconvolution of co-eluting Pep1(N)-OH, Pep1(D)-Am, and Pep1(D_{iso})-Am using the ETD diagnostic ions $(c3 + 57)^+$ of Pep1(D_{iso})-Am and $c5^+$ of Pep1(N)-OH. When applied to mixed samples, this approach achieved overall mean absolute deviations <5% for most species and <10% for Pep1(D_{iso})-Am

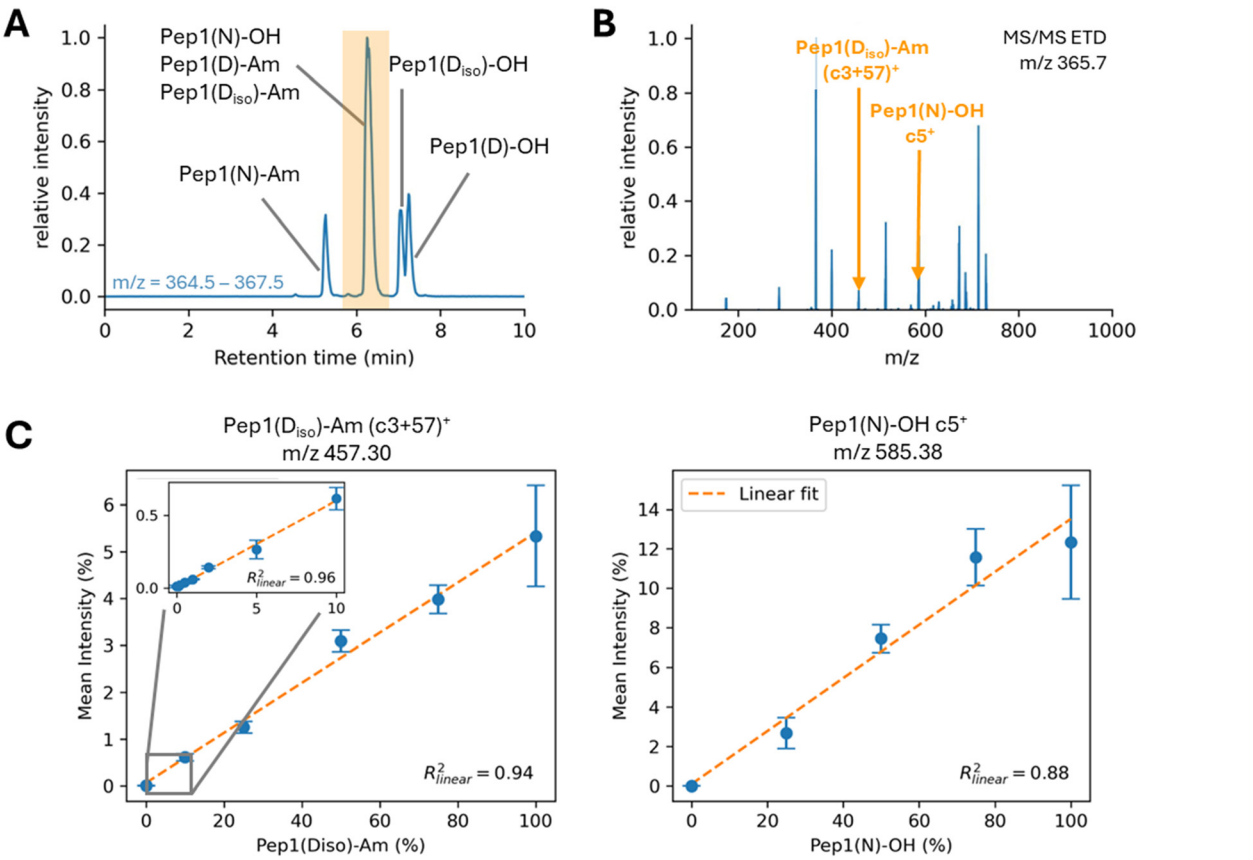

Fig. 2 (A) Extracted ion chromatogram in the *m/z* range 364.5–367.5 acquired with 0.1% FA in H_2O/ACN using a 1% min^{-1} gradient from 98% H_2O at 25 °C. Coeluting peptides Pep1(N)-OH, Pep1(D)-Am, and Pep1(D_{iso})-Am are highlighted in orange. (B) ETD spectrum of $[M + 2H]^{2+}$ precursor of co-eluting peptides Pep1(N)-OH, Pep1(D)-am, and Pep1(D_{iso})-am with diagnostic ions $(c3 + 57)^+$ for Pep1(D_{iso})-am and $c5^+$ for Pep1(N)-OH indicated. (C) Linear fits showing the correlation between signal intensity and peptide content with according R^2 for Pep1(D_{iso})-Am and Pep1(N)-OH in mixtures with Pep1(D)-Am.

Absolute and relative accuracy of the content determination of Pep1(N)-OH are given in the SI (Fig. S4), providing sufficient accuracy for semiquantitative analysis of deamidation and isoAsp formation. Although the relative design means that errors propagate across components, the workflow was shown to be robust against variation in absolute sample concentration and injection volume. Notably, the distinction of individual peptide forms was achieved using a low-resolution mass spectrometer, demonstrating that high mass resolving power is not a prerequisite when informative fragment ions are available. While the diagnostic fragments identified here are sequence-specific, and their general applicability across different peptides remains to be evaluated, this proof-of-concept demonstrates that reliable semiquantitative discrimination can be achieved for closely related peptide variants using MS/MS readouts even in the absence of prior chromatographic separation.

3.2 Detection of deamidation and isoaspartate formation in different solvents

We next applied the workflow to monitor deamidation and isoaspartate formation of Pep1(N)-Am across solvents and conditions over time. Time courses of %-content are summarized in Fig. 3. Full datasets are provided in the SI (Fig. S4). In neutral aqueous media, including water, water/organic mixtures and 10 mM NaCl, Pep1(N)-Am remained unchanged over the study period. In contrast, incubation in PBS (pH 7.4) led to the time-dependent formation of Pep1(D_{iso})-Am with minimal direct deamidation, consistent with the succinimide pathway favoured near neutral pH and confirming the sensitivity of the diagnostic-ion readout. Acidic solutions (0.1% AA, 0.1% FA, 0.1% TFA, 10 mM HCl) promoted deamidation and yielded predominantly Pep1(N)-OH, with no detectable isoAsp formation.

The apparent rate increased with acidity (AA < FA < TFA < HCl) and with temperature: degradation was pronounced at 60 °C, slower at 20 °C, and negligible at 4 °C and −20 °C, the latter also with included freeze–thaw cycles. These observations indicate that cold storage effectively suppresses acid-driven hydrolysis on the timescale studied. Because TFA is widely used in peptide purification, we examined a concentration series. Increasing TFA from 0.1% to 0.2% approximately doubled the extent of deamidation (Fig. 3). At 5% TFA, conversion

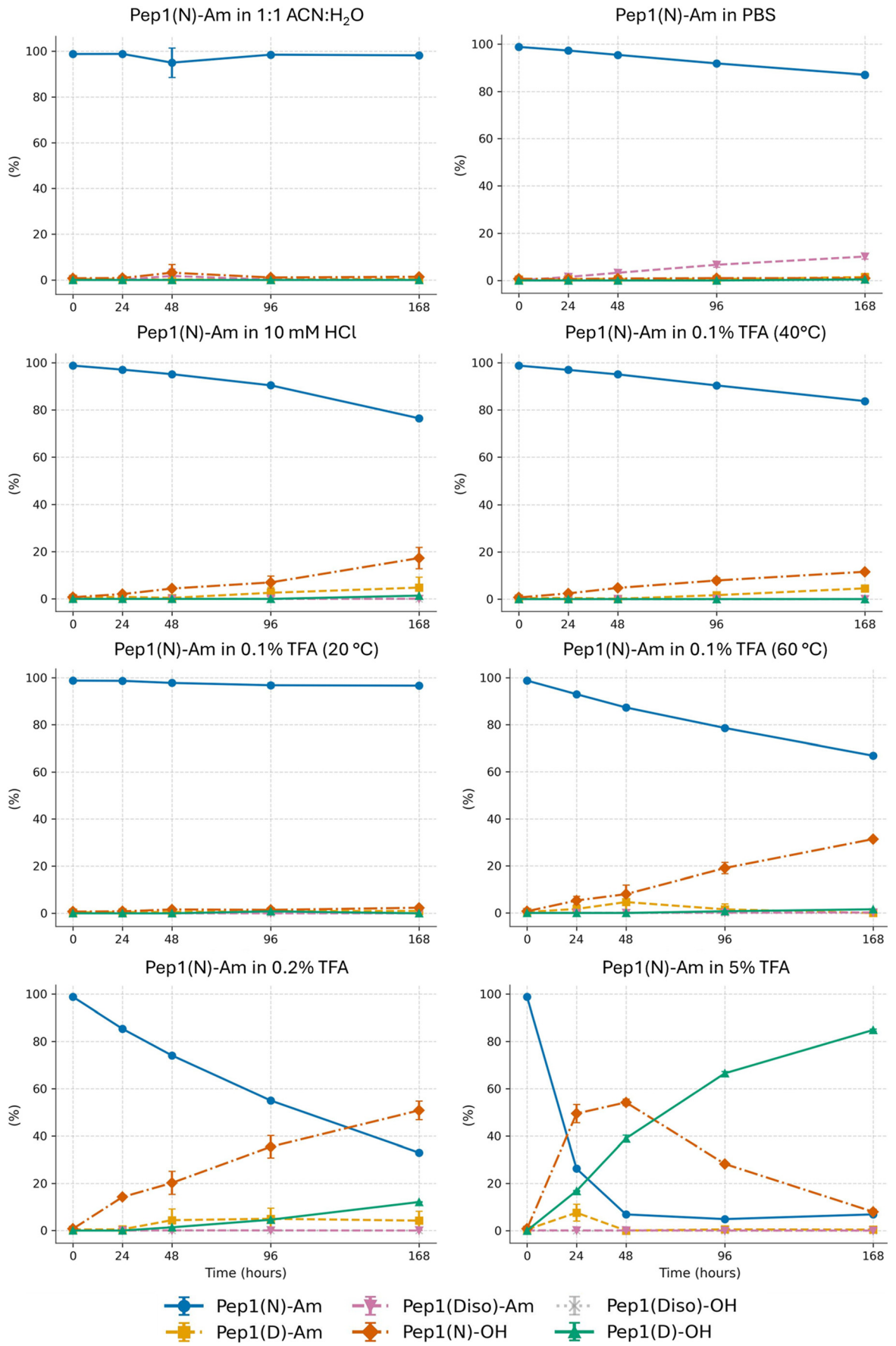

Fig. 3 Relative content of deamidated species over time after incubation of Pep1(N)-Am in different solvents at 40 °C if not stated otherwise.

was substantial and Pep1(D)-OH became the dominant species after seven days. At 50% TFA, degradation accelerated further and the parent peptide was largely depleted, accompanied by additional signals outside the monitored *m*/*z* window that likely reflect secondary reactions (Fig. S4). Exposure to mildly basic solutions (0.1% NH_3, 0.1% DIPEA) led to the appearance of several additional species, with Pep1(D_{iso})-Am becoming a dominant product in 0.1% NH_3, as expected for isoAsp formation under basic conditions. In contrast, nearly anhydrous (100%) TFA caused no detectable deamidation, highlighting the requirement for water. High-TFA samples consistently showed an additional peak at 2.6 min with the same nominal mass as Pep1(N)-Am, whose identity remains unclear and requires further investigation. Selected chromatograms for degradation profiling are shown in Fig. 4. All further chromatograms are given in the SI (Fig. S4).

Other unexpected signals with the same nominal *m*/*z* as the starting material were also observed. These could reflect partial epimerization to D-residue-containing species, a known base-promoted side reaction, although this requires confirmation by comparison to synthesized reference compounds. In 0.1% NaOH, Pep1(N)-Am was no longer detectable at later time points, consistent with rapid base-catalyzed degradation. Structural elucidation of the unknown products will require further analysis by untargeted MS/MS analysis.

3.3 C-terminal amide and glutamine side-chain stability under mildly acidic conditions

To confirm whether the C-terminal amide is more labile than the Asn side-chain amide, we examined peptides containing only one amide functionality: Pep1(D)-Am (C-terminal amide) and Pep1(N)-OH (Asn side-chain amide), using Pep1(D)-OH as a control. Under 0.2% TFA at 40 °C, Pep1(D)-Am deamidated more rapidly than Pep1(N)-OH, as reflected by the faster accumulation of Pep1(D)-OH over time (Fig. 5). This could indicate greater solvent accessibility of the terminus, whereas the side-chain amide may be involved in stabilizing interactions, however this needs further investigation.

We next assessed whether the glutamine side-chain amide shows similar reactivity under mildly acidic conditions. In 0.2% TFA, the Gln-containing analog showed a clear time-dependent formation of deamidated products (Fig. 5), indicating that solvent-dependent direct hydrolysis affects Gln residues similarly to Asn. MS/MS analysis of the individual peaks (Table S2) supports their assignment as Pep1(E)-Am, Pep1(Q)-OH, and Pep1(E)-OH, although full structural confirmation will require synthesized reference standards. These results demonstrate that direct hydrolysis in mildly acidic media impacts all amide functional groups (Fig. 6).

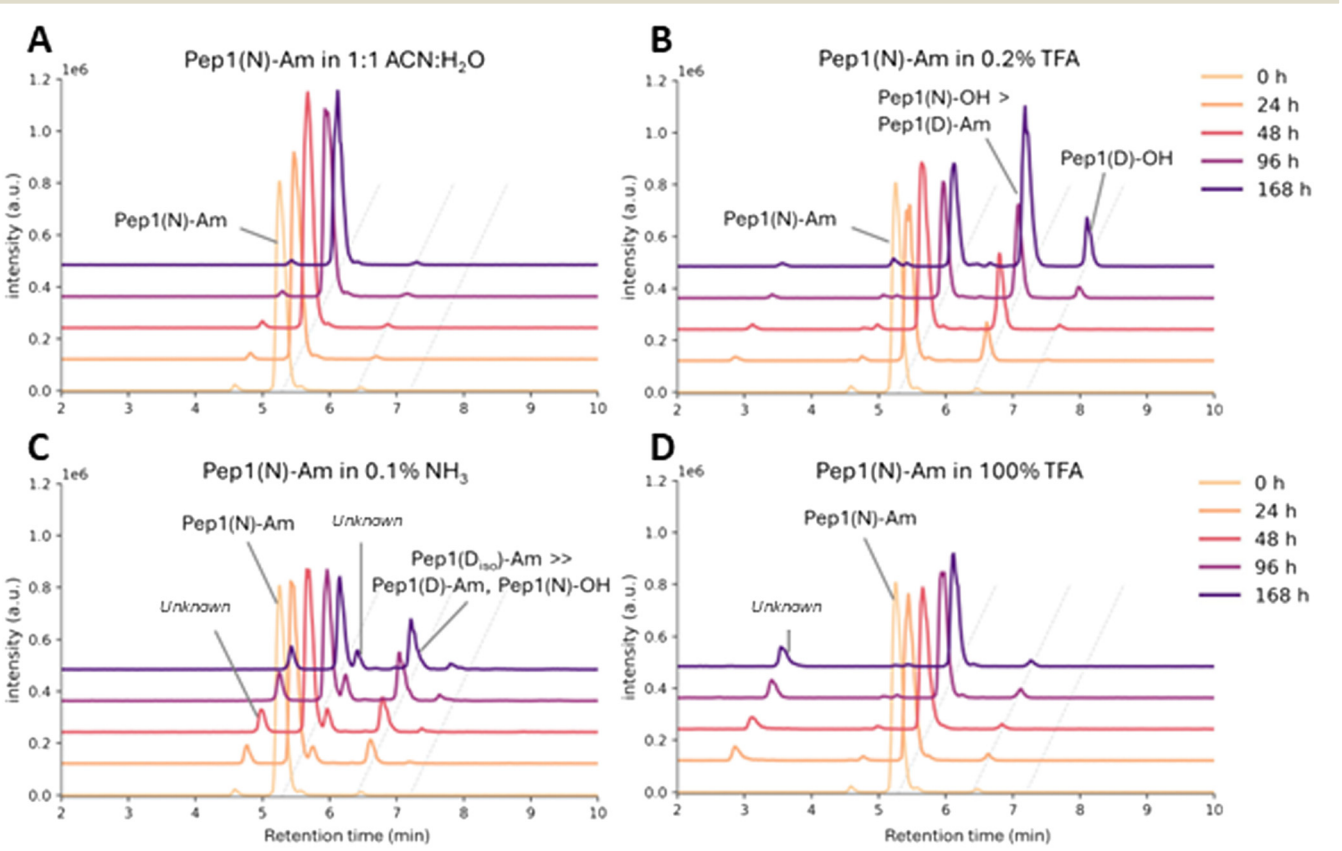

Fig. 4 LC-MS chromatograms [*m*/*z* range 364.5–367.5] show the degradation of Pep1(N)-Am under different conditions: A) 1 : 1 ACN : H_2O; B) 0.2% TFA; C) 0.1% NH_3; D) 100% TFA.

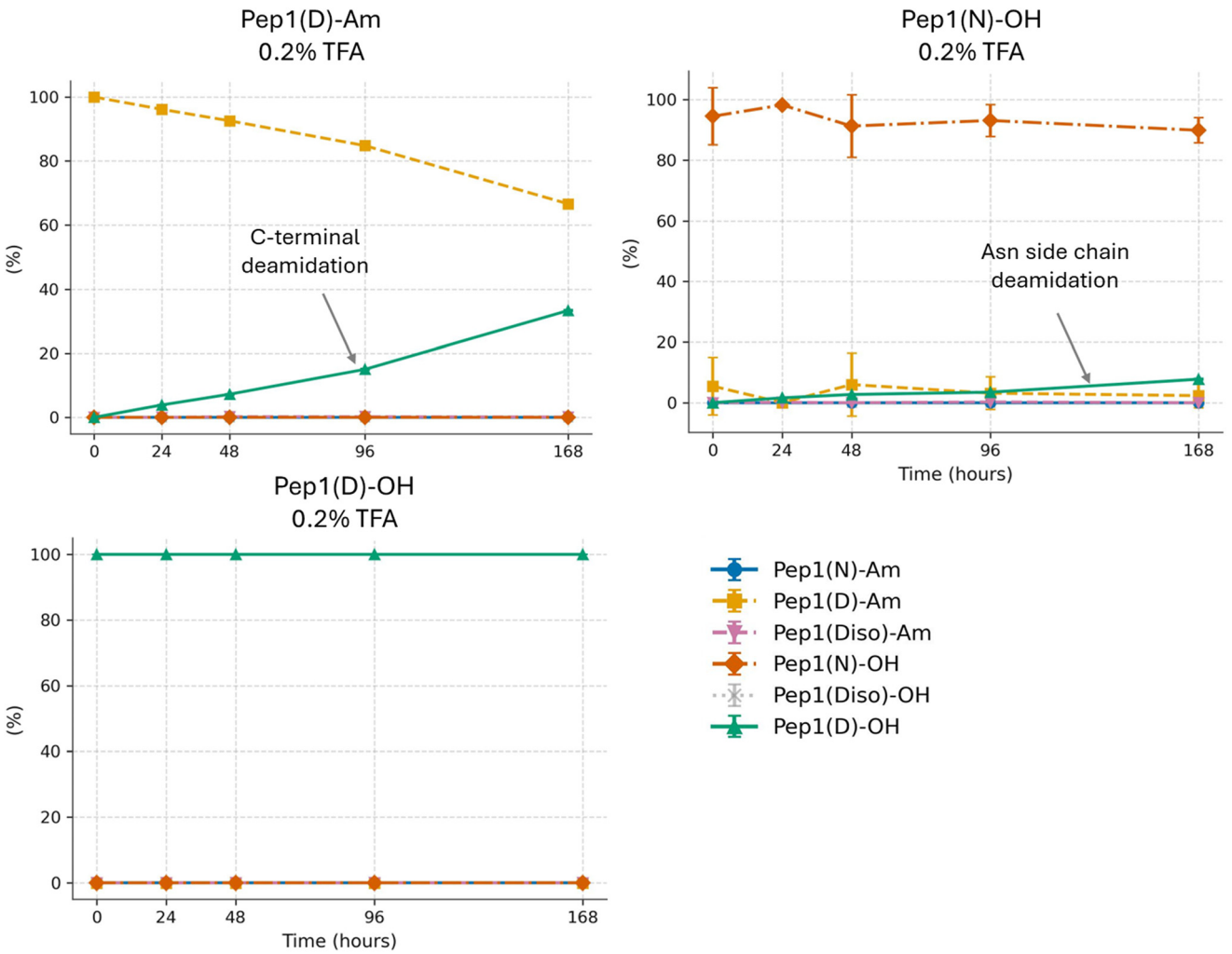

Fig. 5 Deamidation of Pep1(D)-Am, Pep1(N)-OH and Pep1(D)-OH in 0.2% TFA at 40 °C over time.

Conclusion and outlook

In this work, we showed that common RPLC-ESI-MS/MS, without specialized columns and/or optimized chromatographic separation strategies can deliver semiquantitative information on deamidation and isoAsp formation even when key species co-elute. By combining extracted-ion peak integration for LC-resolved components with diagnostic fragment-ion readouts for overlaps, the method achieved 5–10% absolute accuracy under routine settings. Applied to Pep1(N)-Am, the observed condition trends are consistent. At near neutral pH (PBS), isoAsp accumulates suggesting degradation *via* the succinimide pathway, while in aqueous acidic media, primarily direct hydrolysis was observed. Accumulation rate of Pep1(N)-OH increased with acidity and temperature. For TFA-containing solutions, both the TFA concentration and the water content influenced the outcome. Low-percentage aqueous TFA accelerates deamidation, whereas nearly anhydrous TFA shows little to no conversion. Basic media rapidly degraded the peptide, generating additional pathways beyond the targeted readout that will require deeper analysis. Interestingly, in our experiments the C-terminal amide was more labile under acidic conditions compared to the Asn side-chain amide, which could reflect solvent accessibility but requires further investigation. Gln showed similar

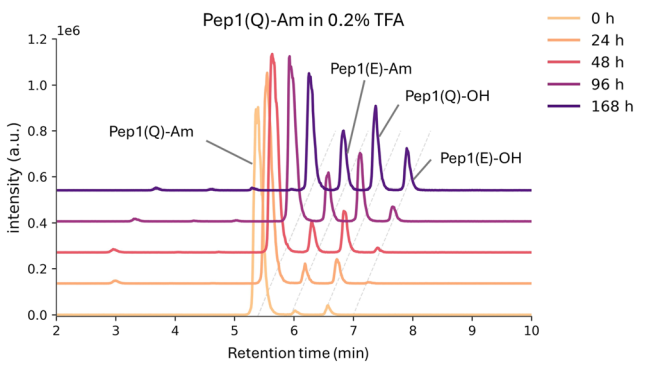

Fig. 6 Overlap of chromatograms obtained from different timepoints after Pep1(Q)-Am incubation in 0.2% TFA at 40 °C. Deamidation products detected and analysed by MS/MS are indicated.

behavior to Asn under these conditions. Importantly, these reactions occur in solvents and additives routinely used for peptide analysis, purification, and storage (*e.g.*, aqueous TFA, FA/AA modifiers, PBS), highlighting the broader relevance of our observations for amidated peptides. Future work could expand to a broader set of amidated peptides to assess differences between side-chain and terminal amides and to evaluate their involvement in local secondary structure influences their reactivity. Although this study intentionally stayed within routine peptide workflows, orthogonal chromatographic separations (*e.g.*, alternative pH, different stationary phases, HILIC) could resolve overlaps and reduce reliance on fragment readouts, and additional fragmentation methods such as EAD or UVPD may broaden diagnostic coverage and enable more refined quantification.

Author contributions

V. E. designed the experiments, synthesized and purified peptides, performed LC-MS/MS and stability experiments, conducted data evaluation, prepared figures and tables and wrote the manuscript. L. C. R. and A. M. synthesized and purified peptides and performed initial proof of concept stability and LC-MS/MS experiments. C. S. supervised the project, was responsible for the resources and wrote the manuscript. All authors read and reviewed the final version of the manuscript.

Conflicts of interest

There is no conflict of interest to report.

Data availability

The data supporting this article (MS spectra, LC-UV-, LC-MS chromatograms) have been included as part of the supplementary information (SI). Other data are available from the corresponding authors upon request.

Supplementary information is available. See DOI: https://doi.org/10.1039/d5md01025j.

Acknowledgements

We are grateful to Alessandro Streuli and Joshua Meyer for their insightful and inspiring scientific discussions as well as Ina Schmidt for the instrumental support. We also thank the laboratory of Gisbert Schneider for providing access to the peptide synthesizer and freeze-drying facility. The graphical abstract was created in BioRender. Steuer, C. (2026) https://BioRender.com/v3r5dmb. The authors thank ETH Zurich for covering the Open Access publication costs.

References

1 A. Henninot, J. C. Collins and J. M. Nuss, The Current State of Peptide Drug Discovery: Back to the Future?, *J. Med. Chem.*, 2018, **61**(4), 1382–1414, DOI: 10.1021/acs.jmedchem.7b00318.

2 C. L. Gare, A. M. White and L. R. Malins, From lead to market: chemical approaches to transform peptides into therapeutics, *Trends Biochem. Sci.*, 2025, **50**(6), 467–480, DOI: 10.1016/j.tibs.2025.01.009.

3 V. D'Aloisio, P. Dognini, G. A. Hutcheon and C. R. Coxon, PepTherDia: database and structural composition analysis of approved peptide therapeutics and diagnostics, *Drug Discovery Today*, 2021, **26**(6), 1409–1419, DOI: 10.1016/j.drudis.2021.02.019.

4 C. Morrison, Constrained peptides' time to shine?, *Nat. Rev. Drug Discovery*, 2018, **17**(8), 531–533, DOI: 10.1038/nrd.2018.125.

5 V. Erckes, A. Streuli, L. Chamera Rendueles, S. D. Krämer and C. Steuer, Towards a Consensus for the Analysis and Exchange of TFA as a Counterion in Synthetic Peptides and Its Influence on Membrane Permeation, *Pharmaceuticals*, 2025, **18**, 1163–1179, DOI: 10.3390/ph18081163.

6 A. Boudier-Lemosquet, A. Mahler, C. Bobo, M. Dufossée and M. Priault, Introducing protein deamidation: Landmark discoveries, societal outreach, and tentative priming workflow to address deamidation, *Methods*, 2022, **200**, 3–14, DOI: 10.1016/j.ymeth.2021.11.012.

7 H. Yokoyama, R. Mizutani, S. Noguchi and N. Hayashida, Structural and biochemical basis of the formation of isoaspartate in the complementarity-determining region of antibody 64M-5 Fab, *Sci. Rep.*, 2019, **9**(1), 18494, DOI: 10.1038/s41598-019-54918-0.

8 S. R. Dennison, L. H. G. Morton, K. Badiani, F. Harris and D. A. Phoenix, The effect of C-terminal deamidation on bacterial susceptibility and resistance to modelin-5, *Eur. Biophys. J.*, 2025, **54**(1–2), 45–63, DOI: 10.1007/s00249-025-01732-4, From NLM.

9 D. J. Merkler, C-Terminal amidated peptides: Production by the in vitro enzymatic amidation of glycine-extended peptides and the importance of the amide to bioactivity, *Enzyme Microb. Technol.*, 1994, **16**(6), 450–456, DOI: 10.1016/0141-0229(94)90014-0.

10 M. Lang, R. M. Söll, F. Dürrenberger, F. M. Dautzenberg and A. G. Beck-Sickinger, Structure–Activity Studies of Orexin A and Orexin B at the Human Orexin 1 and Orexin 2 Receptors Led to Orexin 2 Receptor Selective and Orexin 1 Receptor Preferring Ligands, *J. Med. Chem.*, 2004, **47**(5), 1153–1160, DOI: 10.1021/jm030982t.

11 V. A. Adegoke, Y. Dongol, T. Gonzalez, A. Song, R. J. Clark, R. J. Lewis, A. C. Conibear, K. J. Rosengren and M. Aguilar, Proline hydroxylation and C-terminal amidation in μ-conotoxins increase structural stability and potency at sodium channels, *Aust. J. Chem.*, 2025, **78**(9), 25071–25081, DOI: 10.1071/CH25071.

12 S. Catak, G. Monard, V. Aviyente and M. F. Ruiz-López, Deamidation of Asparagine Residues: Direct Hydrolysis versus Succinimide-Mediated Deamidation Mechanisms, *J. Phys. Chem. A*, 2009, **113**(6), 1111–1120, DOI: 10.1021/jp808597v.

13 D. W. Aswad, M. V. Paranandi and B. T. Schurter, Isoaspartate in peptides and proteins: formation, significance, and analysis, *J. Pharm. Biomed. Anal.*, 2000, **21**(6), 1129–1136, DOI: 10.1016/S0731-7085(99)00230-7.

14 H. T. Wright, Sequence and structure determinants of the nonenzymatic deamidation of asparagine and glutamine residues in proteins, *Protein Eng.*, 1991, **4**(3), 283–294, DOI: 10.1093/protein/4.3.283, (accessed 9/16/2025).

15 K. Neumann, J. Farnung, S. Baldauf and J. W. Bode, Prevention of aspartimide formation during peptide synthesis using cyanosulfurylides as carboxylic acid-protecting groups, *Nat. Commun.*, 2020, **11**(1), 982, DOI: 10.1038/s41467-020-14755-6.

16 N. E. Robinson and A. B. Robinson, Molecular clocks, *Proc. Natl. Acad. Sci. U. S. A.*, 2001, **98**(3), 944–949, DOI: 10.1073/pnas.98.3.944.

17 E. Logerot, C. Perrin, Y. Ladner, F. Aubriet, V. Carré and C. Enjalbal, Quantitating α-amidated peptide degradation by separative technologies and ultra-high resolution mass spectrometry, *Talanta*, 2023, **253**, 124036, DOI: 10.1016/j.talanta.2022.124036.

18 E. Logerot, G. Cazals, A. Memboeuf and C. Enjalbal, Revealing C-terminal peptide amidation by the use of the survival yield technique, *Anal. Biochem.*, 2022, **655**, 114823, DOI: 10.1016/j.ab.2022.114823.

19 K. F. Medzihradszky and R. J. Chalkley, Lessons in de novo peptide sequencing by tandem mass spectrometry, *Mass Spectrom. Rev.*, 2015, **34**(1), 43–63, DOI: 10.1002/mas.21406, From NLM Medline.

20 H. Steen and M. Mann, The abc's (and xyz's) of peptide sequencing, *Nat. Rev. Mol. Cell Biol.*, 2004, **5**(9), 699–711, DOI: 10.1038/nrm1468.

21 J. E. Syka, J. J. Coon, M. J. Schroeder, J. Shabanowitz and D. F. Hunt, Peptide and protein sequence analysis by electron transfer dissociation mass spectrometry, *Proc. Natl. Acad. Sci. U. S. A.*, 2004, **101**(26), 9528–9533, DOI: 10.1073/pnas.0402700101.

22 Y. Yamazaki, N. Fujii, Y. Sadakane and N. Fujii, Differentiation and Semiquantitative Analysis of an Isoaspartic Acid in Human α-Crystallin by Postsource Decay in a Curved Field Reflectron, *Anal. Chem.*, 2010, **82**(15), 6384–6394, DOI: 10.1021/ac100310x.

23 P. Schindler, D. Müller, W. Märki, H. Grossenbacher and W. J. Richter, Characterization of a β-Asp33 Isoform of Recombinant Hirudin Sequence Variant 1 by Low-energy Collision-induced Dissociation, *J. Mass Spectrom.*, 1996, **31**(9), 967–974, DOI: 10.1002/(SICI)1096-9888(199609)31:9<967::AID-JMS381>3.0.CO;2-K, (accessed 2025/09/12).

24 L. J. González, T. Shimizu, Y. Satomi, L. Betancourt, V. Besada, G. Padrón, R. Orlando, T. Shirasawa, Y. Shimonishi and T. Takao, Differentiating α- and β-aspartic acids by electrospray ionization and low-energy tandem mass spectrometry, *Rapid Commun. Mass Spectrom.*, 2000, **14**(22), 2092–2102, DOI: 10.1002/1097-0231(20001130)14:22<2092::AID-RCM137>3.0.CO;2-V, (accessed 2025/09/12).

25 J. Martens, G. Berden and J. Oomens, Structures of Fluoranthene Reagent Anions Used in Electron Transfer Dissociation and Proton Transfer Reaction Tandem Mass Spectrometry, *Anal. Chem.*, 2016, **88**(12), 6126–6129, DOI: 10.1021/acs.analchem.6b01483.

26 P. B. O'Connor, J. J. Cournoyer, S. J. Pitteri, P. A. Chrisman and S. A. McLuckey, Differentiation of Aspartic and Isoaspartic Acids Using Electron Transfer Dissociation, *J. Am. Soc. Mass Spectrom.*, 2006, **17**(1), 15–19, DOI: 10.1016/j.jasms.2005.08.019.

27 N. DeGraan-Weber, J. Zhang and J. P. Reilly, Distinguishing Aspartic and Isoaspartic Acids in Peptides by Several Mass Spectrometric Fragmentation Methods, *J. Am. Soc. Mass Spectrom.*, 2016, **27**(12), 2041–2053, DOI: 10.1007/s13361-016-1487-9.

28 V. Erckes, M. Hilleke, C. Isert and C. Steuer, PICKAPEP: An application for parameter calculation and visualization of cyclized and modified peptidomimetics, *J. Pept. Sci.*, 2024, **30**(12), e3646, DOI: 10.1002/psc.3646.

29 R. Adusumilli and P. Mallick, Data Conversion with ProteoWizard msConvert, in *Proteomics: Methods and Protocols*, ed. L. Comai, J. E. Katz and P. Mallick, Springer New York, 2017, pp. 339–368.

30 M. C. Chambers, B. Maclean, R. Burke, D. Amodei, D. L. Ruderman, S. Neumann, L. Gatto, B. Fischer, B. Pratt and J. Egertson, *et al.*, A cross-platform toolkit for mass spectrometry and proteomics, *Nat. Biotechnol.*, 2012, **30**(10), 918–920, DOI: 10.1038/nbt.2377.

31 *The Python Language Reference*, https://docs.python.org/3/reference/, (accessed January 22, 2024).

32 H. L. Röst, U. Schmitt, R. Aebersold and L. Malmström, pyOpenMS: A Python-based interface to the OpenMS mass-spectrometry algorithm library, *Proteomics*, 2014, **14**(1), 74–77, DOI: 10.1002/pmic.201300246.

33 C. P. Haas, M. Lübbesmeyer, E. H. Jin, M. A. McDonald, B. A. Koscher, N. Guimond, L. Di Rocco, H. Kayser, S. Leweke and S. Niedenführ, *et al.*, Open-Source Chromatographic Data Analysis for Reaction Optimization and Screening, *ACS Cent. Sci.*, 2023, **9**(2), 307–317, DOI: 10.1021/acscentsci.2c01042.

34 C. R. Harris, K. J. Millman, S. J. van der Walt, R. Gommers, P. Virtanen, D. Cournapeau, E. Wieser, J. Taylor, S. Berg and N. J. Smith, *et al.*, Array programming with NumPy, *Nature*, 2020, **585**(7825), 357–362, DOI: 10.1038/s41586-020-2649-2.

35 *pandas User Guide*, https://pandas.pydata.org/, (accessed January 22, 2024).

36 *SciPy*, https://scipy.org/, (accessed 23.08.2024).

37 *Matplotlib*, https://matplotlib.org/, (accessed 23.08.24).

38 B. J. Bythell, S. Suhai, Á. Somogyi and B. Paizs, Proton-Driven Amide Bond-Cleavage Pathways of Gas-Phase Peptide Ions Lacking Mobile Protons, *J. Am. Chem. Soc.*, 2009, **131**(39), 14057–14065, DOI: 10.1021/ja903883z.

39 M. Dupré, S. Cantel, J. Martinez and C. Enjalbal, Occurrence of C-Terminal Residue Exclusion in Peptide Fragmentation

by ESI and MALDI Tandem Mass Spectrometry, *J. Am. Soc. Mass Spectrom.*, 2012, **23**(2), 330–346, DOI: 10.1007/s13361-011-0254-1.

40 B. Paizs and S. Suhai, Fragmentation pathways of protonated peptides, *Mass Spectrom. Rev.*, 2005, **24**(4), 508–548, DOI: 10.1002/mas.20024.